

### RAPID COMMUNICATIONS

*Rapid Communications are intended for the accelerated publication of important new results and are therefore given priority treatment both in the editorial office and in production. A Rapid Communication in Physical Review B may be no longer than four printed pages and must be accompanied by an abstract. Page proofs are sent to authors.*

#### **Fast *in situ* x-ray-diffraction studies of chemical reactions: A synchrotron view of the hydration of tricalcium aluminate**

A. C. Jupe, X. Turrillas, P. Barnes,\* and S. L. Colston

*Industrial Materials Group, Department of Crystallography, Birkbeck College, Malet Street, London WC1E 7HX, United Kingdom*

C. Hall

*Schlumberger Cambridge Research, High Cross, Madingley Road, Cambridge CB3 0EL, United Kingdom*

D. Häusermann and M. Hanfland

*European Synchrotron Radiation Facility, Boîte Postale 220, F-38043 Grenoble, France*

(Received 22 January 1996; revised manuscript received 21 March 1996)

We report observations on the early hydration of tricalcium aluminate, the most reactive component of Portland cement, using rapid-energy dispersive diffraction on a high brilliance synchrotron source. *In situ* observations of the hydration process over short time scales, and through bulk samples, reveal an intermediate calcium aluminate hydrate appearing just prior to the formation of the final stable hydrate, demonstrating the nucleating role of this intermediate. The superior quality of the data is sufficient to yield concentration versus time plots for each phase over the whole hydration sequence. This improvement derives from being able to use smaller diffracting volumes and consequent removal of time smearing due to inhomogenetics, and thus now offers the possibility of extending the technique in terms of time resolution and diversity of system. [S0163-1829(96)51022-2]

Third generation synchrotron radiation sources are now providing intense beams of high-energy x-ray photons with collimation characteristics that can be exploited in the study of reactions within bulk solid state materials. For example, the European Synchrotron Radiation Facility (ESRF) has a source size of circa  $120 \times 250 \mu\text{m}$ , a very high brilliance and usable energies up to 200 keV for diffraction purposes. In the studies reported here the samples were exposed to fluxes of the order of  $10^{12}$  photons per second per  $\text{mm}^2$  in a 0.1% bandwidth at 50 keV. This represents an increase of 50–100 compared to equivalent experimental fluxes using second generation sources.

Given these features we can now use synchrotron methods to look at much faster solid-state transformations than previously. The hydration of Portland cement, the reactive binder in concretes<sup>1</sup> for construction and in grouts for oil field engineering,<sup>2</sup> at first appears to be slow, reacting with water on a time scale of hours and developing final strength over many months.<sup>3,4</sup> Nevertheless there is evidence, such as

from adiabatic calorimetry<sup>5</sup> and environmental scanning electron microscopy,<sup>6</sup> of some intense chemical and microstructural activity over the first few minutes following the initial contact between water and the anhydrous cement. However the direct observation of critical rapid mineralogical changes in dense cement pastes on the time scale of seconds has only now become possible by use of the latest synchrotron technology.

It has long been known<sup>4,7</sup> that the early hydration of Portland cement, i.e., the first few hours after mixing with water, is greatly influenced by the behavior of its most reactive component, tricalcium aluminate, or “C<sub>3</sub>A” for short. Its hydration reactions can be conveniently expressed using a cement chemistry shorthand (e.g., see Taylor<sup>7,8</sup>) in which the various phases are written in terms of the oxides (C=CaO; A=Al<sub>2</sub>O<sub>3</sub>; H=H<sub>2</sub>O). Using this shorthand, we can summarize key parts of the hydration process in terms of the formation of several hydrates

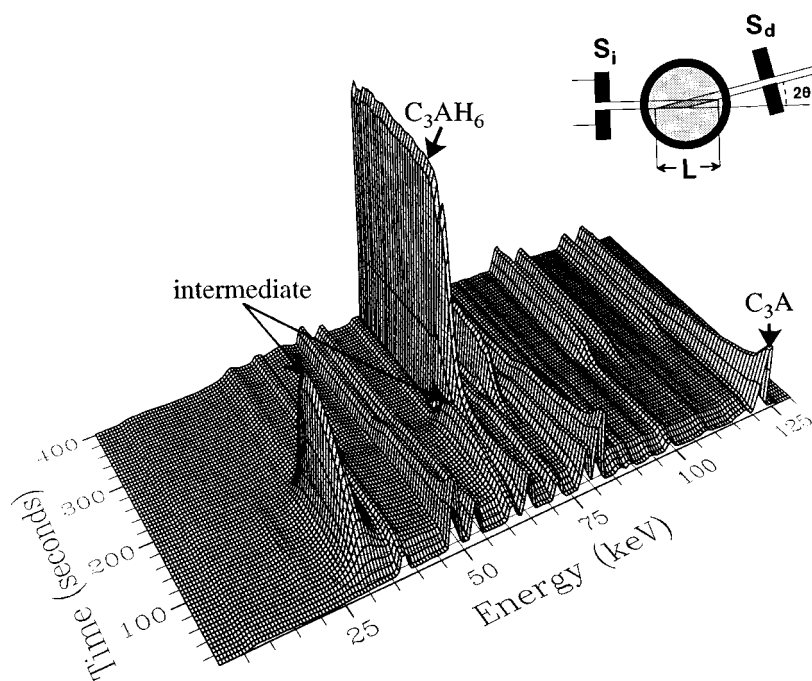
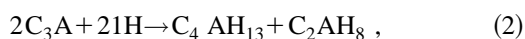
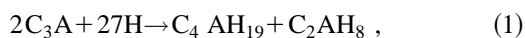


FIG. 1. Time-resolved energy dispersive diffraction patterns showing the rapid hydration of tricalcium aluminate from the moment of water addition. Each pattern here has been collected over 5 s the photon count rate being 29 kcps. The tricalcium aluminate (prominent peaks near 50, 80, and 120 keV) starts to be consumed almost immediately followed by the growth of the intermediate phase (main peaks near 30 and 60 keV); after about 200 s the intermediate phase disappears abruptly and simultaneously with the commencement of rapid growth of the stable hydrate  $C_3AH_6$  (main peaks near 65 and 75 keV). The inset illustrates the basic geometry of the energy-dispersive diffractometer in plan view: the incident beam is defined by the first slit  $S_i$ ; the diffracted beam is defined at an angle  $2\theta$  by the second slit  $S_d$ ; the overall slit system also defines a precise region, termed a ‘‘diffraction lozenge’’ of length  $L$ , from which diffracted x-ray photons reach the detector (not shown) to form the eventual energy-dispersive diffraction patterns.



Of these hydrates  $C_3AH_6$  is the most stable, particularly at high temperatures. In fact the hydration of  $C_3A$  is notoriously variable and rapid, so much so that reactions such as (1)–(3) can lead to a condition known as ‘‘flash set’’; this is avoided by the addition of mineral gypsum,  $CaSO_4 \cdot 2H_2O$ , to most cements during manufacture to provide a source of soluble sulphate ions which appear to suppress formation of calcium aluminate hydrates and rather divert the reaction pathway towards formation of a complex calcium sulphoaluminate hydrate mineral known as ettringite (e.g., see Jawed *et al.*<sup>4</sup>).

The attributes of synchrotron energy dispersive diffraction for studying chemical reactions have already been detailed.<sup>9–13</sup> Briefly these are: using the *continuous* synchrotron x-ray spectrum at a fixed collection angle ( $2\theta$ ) simplifies the design of environmental sample cells; by using low- $2\theta$  collection angles the diffraction peaks occur at high energies and this gives rise to x-ray penetrations three orders of magnitude greater than with conventional laboratory sources, enabling bulk samples to be examined (e.g., 8–12 mm thicknesses for cements); the high intensity can be harnessed to yield time-resolved diffraction patterns on time scales of seconds. These attributes are enhanced further by third generation sources: The intensity increase not only permits shorter collection times but also permits reduction of the beam size defining slits so that the pattern resolution becomes less degraded by geometrical effects. Since low- $2\theta$ -angles are essential for x-ray penetration through bulk samples, yet confer a serious broadening effect proportional to  $\cot\theta$  ( $\cot\theta = 52$  for  $2\theta = 2.2^\circ$  in these studies), this is a significant enhancement for complex powder patterns such as with cement; however, there is a further important enhancement which has

arisen from using reduced defining slits, which is that a much smaller effective diffraction volume is defined and this has the quite unexpected effect of decisively sharpening the realized time resolution, as explained later. Finally, the increase in photon flux at high energies effectively extends the energy range of the diffraction patterns.

In the experiments reported here, we used a sample container in the form of a polymer PEEK (poly ether-ether ketone) cylindrical cell (8 mm internal diameter by 40 mm length). This cell was initially filled with unreacted  $C_3A$  (tricalcium aluminate) to which water was added by means of a remotely operated syringe which thus enabled data collection to begin before the start of hydration without loss of valuable time performing x-ray safety search procedures. The diffractometer  $2\theta$  angle was set at  $2.2^\circ$ , a primary x-ray beam of 0.45 mm (vertical) by 0.05 mm (horizontal) was incident on the sample, and a diffracted beam slit of 0.08 mm vertical separation effectively defined<sup>12</sup> the diffraction volume within the sample (see insert in Fig. 1) in the shape of a discoid of around  $0.1 \text{ mm}^3$  volume spread across the 8 mm diameter of the *spinning* cylindrical specimen cell tube. During data collection the sample was spun at 60 rpm on its cylindrical axis to minimize effects of preferred orientation and increase crystallite sampling. The white x-ray beam has to pass through the sample cell walls in addition to the 8 mm of sample ( $C_3A + \text{water}$ ) within, though reasonable diffraction intensities were still possible on account of the intense synchrotron beam and lower absorption of x rays at the energies used. With such penetration we can be assured that bulk (internal) material is being sampled, compared to the near-surface sampling (e.g., depths  $< 100 \mu\text{m}$ ) with laboratory diffractometers.

The  $C_3A$  and added water were both equilibrated initially to ambient temperature ( $26^\circ\text{C}$ ). However, the cement, in addition to undergoing an exothermic hydration reaction, is also heated locally by the synchrotron beam which has a power density of approximately  $15 \text{ W mm}^{-2}$  even after 0.1

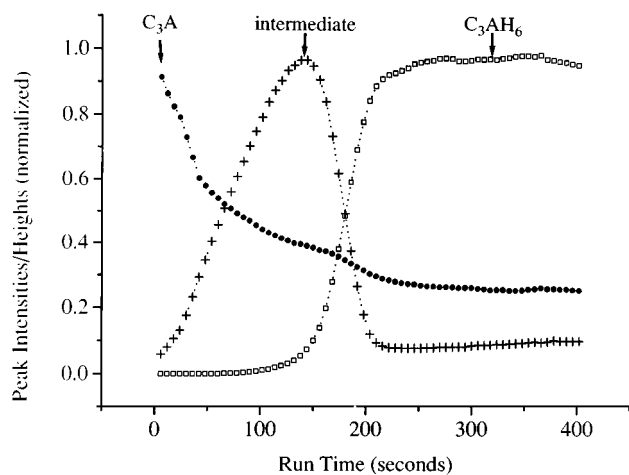


FIG. 2. Quantitative phase versus time plots for the hydration sequence in Fig. 1, obtained by peak fitting and area calculations (peak intensity) to the best resolved peaks for the  $C_3A$  (440 peak at  $2.699 \text{ \AA}/119.67 \text{ keV}$ ) and  $C_3AH_6$  (220 peak at  $4.442 \text{ \AA}/72.71 \text{ keV}$ ), and by the height of the  $10.7 \text{ \AA}$  peak for the intermediate phase due to its irregular peak shape. Values are normalized so that each phase maximum corresponds to unity. The curves demonstrate the coincidence in loss of  $C_3A$  with growth of intermediate, and loss of intermediate with growth of  $C_3AH_6$ .

mm carbon and 0.25 mm aluminium filters have been placed in the beam to protect the sample. The effect of the beam heating alone is such that localized cement temperatures, as measured by a thermocouple probe, are increased by up to  $10 \text{ }^\circ\text{C}$ . The actual temperature within the fine diffracting volume may be greater than this, though the important factor is that the volume heated by the synchrotron beam is precisely the same volume from which diffraction information is being collected. Also we know that if we deliberately heat samples up to around  $100 \text{ }^\circ\text{C}$ , then the additional heating effect of the synchrotron beam becomes negligible since in calibration experiments<sup>14</sup> using pure ettringite, as a reference material, its decomposition temperature,  $114 \text{ }^\circ\text{C}$ , is reproduced to within  $\pm 1^\circ\text{C}$ .

The results concerning the hydration of tricalcium aluminate are presented in Figs. 1–3 and are now discussed. First the diffraction pattern quality is greatly improved: the strong measurable  $C_3A$  peaks extend out in energy as far as  $121 \text{ keV}$  (see Fig. 1); the peak widths are very acceptable ( $\Delta d/d = 0.6\text{--}0.95\%$  over the energy range  $48\text{--}121 \text{ keV}$ ) and more than twice as sharp as equivalent diffraction peaks collected on the second generation source at the UK Daresbury-SRS.<sup>14</sup> The superior photon flux permits  $5 \text{ s}$  (Fig. 1) and  $0.3 \text{ s}$  (Fig. 3) collection times and superior concentration versus time plots (e.g., Fig. 2) compared to previous studies<sup>10,15–19</sup> on second generation sources. Using the most reactive  $C_3A$  batch (supplied by Henderson<sup>15</sup>) the  $C_3A$ -hydration sequence observed was found to be rapid with detectable changes after  $10\text{--}20 \text{ s}$  from mixing with water. Because of the surprising nature of the observed hydration, the experiment was repeated five times for confirmation. Although the timing of the “start point” varied across these repeats, a similar time-sequence ensued in each case, a typical result being shown in Fig. 1. Here after a brief dormant period of  $10\text{--}20 \text{ seconds}$ , the  $C_3A$  concentration drops

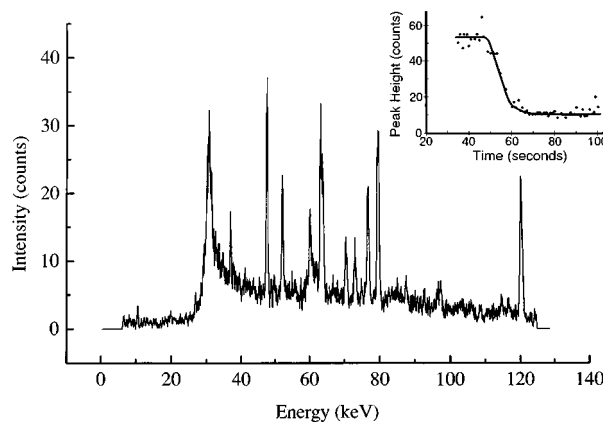


FIG. 3. Typical example of an extremely rapid,  $0.3 \text{ s}$ , energy-dispersive pattern collected during the period while the intermediate phase was disappearing and the  $C_3AH_6$ -final hydrate forming. The inset illustrates the height of one of the intermediate peaks as a function of time (arbitrary zero on time axis), demonstrating the rapidity of this solid-state chemical transition.

as an intermediate phase forms. After  $100\text{--}200 \text{ s}$ , the intermediate phase disappears abruptly as a third phase,  $C_3AH_6$ -hydrate, then forms and thereafter remains. A normalized quantitative plot of the evolution of all three phases versus time is obtained for the whole sequence by integrating appropriate diffraction peaks (see Fig. 2). This clearly shows that the  $C_3AH_6$  does not begin to form until the intermediate reaches its maximum level; then as the intermediate decreases the rate of  $C_3A$  consumption increases slightly, feeding further the formation of  $C_3AH_6$ . In order to track the surprisingly rapid disappearance of this intermediate more closely a further hydration experiment was conducted using a faster data acquisition procedure in which pattern collection times were reduced to  $0.3 \text{ s}$  each spaced by  $0.65 \text{ s}$ . A typical  $0.3 \text{ s}$  diffraction “snapshot,” taken during the period while the intermediate was disappearing, is shown in Fig. 3. An analysis of the intermediate phase’s principal (001) diffraction peak (around  $30 \text{ keV}$ ) demonstrates (insert of Fig. 3) that the intermediate can disappear within about  $10 \text{ s}$ . This is remarkably rapid for an essentially solid state transformation/reaction occurring during cement hydration which is about to enter a so-called “dormant stage” and after which takes months to years to reach completion.

The identification of the intermediate phase is of obvious concern: the two dominant peaks (at  $30.2$  and  $60.4 \text{ keV}$ ) correspond to  $d$  spacings of  $10.7$  and  $5.36 \text{ \AA}$ . Of the well-known hydrates,<sup>7,8</sup> both  $C_2AH_8$  and  $C_4AH_{19}$  match these  $d$  spacings though the intensity ratios fit  $C_2AH_8$  far better than  $C_4AH_{19}$ . In addition a very small peak present at  $3.58 \text{ \AA}$  ( $90.2 \text{ keV}$ ) supports the  $C_2AH_8$  choice. In this respect these results parallel an earlier study by Rashid, Barnes, and Turrillas<sup>17</sup> on the hydrate conversion of  $CAH_{10}$  to  $C_3AH_6$  where  $C_2AH_8$  again appeared as an intermediate phase, though over longer time scales of minutes.

These results represent diffraction observations resulting from the superior time resolution and diffraction pattern quality that were not available during previous cement hydration studies.<sup>10,15–19</sup> They show that the hydration of  $C_3A$  can be rapid, on a  $10\text{--}300 \text{ s}$  time scale, and proceeds

via the necessary intervention of an intermediate crystalline hydrate phase,  $C_2AH_g$ . The data support the idea, previously reported<sup>17</sup> with the much slower conversion reactions, that growth of the final stable  $C_3AH_6$  phase is nucleated by a  $C_2AH_8$ -type intermediate hydrate. It invalidates an older alternative synthesis theory (for example see the general review in Ref. 4) that the  $C_2AH_8$  acts as a *protective* layer around the  $C_3A$  grains, impeding full hydration until the layer becomes “punctured.” If this mechanism were operative the  $C_3A$  loss and  $C_3AH_6$  growth would not be so consistently synchronized with the formation and disappearance of the intermediate phase. Further, these results give us direct clues as to how the addition of gypsum to cements prevents flash set, since we note that when gypsum is added to the cement<sup>14</sup> the formation of ettringite is even more rapid than that of the intermediate. Indeed this must be so if it is to prevent the intermediate from forming and nucleating the  $C_3AH_6$  phase.

We conclude by noting first that this study has revealed one of the fastest ever solid-state multitransformation sequences at bulk/near-ambient conditions. A key feature turns out to be the extremely small diffracting volume within the bulk of the sample. Previously with second generation sources the larger slits brought about both a poorer geometrical resolution and a “time smearing” of diffraction events since unavoidable inhomogeneities in sample, temperature and reactant delivery (e.g., water) resulted in the detector integrating a continuum of similar reaction sequences all slightly displaced in time. In other words, *effective* time resolution is not just a property of the detector system but also

depends on the material and the instrument geometry. Perhaps in hindsight this is not so surprising when we recall that diffraction peak resolution similarly depends on the interplay between instrumental and sample effects. A direct consequence of this effective time-resolution sharpening is that the fleeting presence of the intermediate hydrate, missed previously, has now been clearly captured in this study. The precise sequence of events, free of time-smearing, also unequivocally shows that the intermediate plays a vital nucleating role. It is likely that other reactive transformations in cement hydration also involve intermediates (for example in the decomposition of ettringite<sup>14</sup>). Consequently current ideas on cement hydration are likely to be elaborated and revised. On a more general note, these enhancements open the door to a possible reexamination of many other solid-state/hydrothermal reactions. While it is not suggested that the data quality would necessarily support full rapid time-resolved structure (e.g., Rietveld<sup>20</sup>) refinement, it is certainly sufficient to determine dynamic changes in unit-cell parameters (from around 0.01 to 0.1 %<sup>18</sup>) and to capture short-lived intermediate phases as in this study. It may well be that a similar reexamination of other bulk solid state systems will uncover further intermediate sequences and similarly force us to rethink the mechanisms of reaction chemistry involved.

We thank the EPSRC for project support and the ESRF/SRS for beam time and site-personnel assistance. Also we thank E. Henderson and M. Vickers for specimen acquisition, and C. Morison and T. Bailey for equipment construction.

\*Author to whom correspondence should be addressed.

<sup>1</sup>J. Bensted, in *Advances in Cement Technology*, edited by S.N. Ghose (Pergamon, New York, 1983), p. 307.

<sup>2</sup>K. Luke, C. Hall, T.G.J. Jones, P. Barnes, A.C. Lewis, and X. Turrillas, in *Proceedings of the International Symposium on Oil-field Chemistry*, San Antonio, TX, 1995 (Society of Petroleum Engineers, Richardson, TX, 1995), p. 137.

<sup>3</sup>S. Mindess, in *Structure and Performance of Cements*, edited by P. Barnes (Applied Science, London, 1983), p. 319.

<sup>4</sup>I. Jawed, J. Skalny, and J.F. Young, in *Structure and Performance of Cements* (Ref. 3), p. 267.

<sup>5</sup>D. Damidot, A. Nonat, and P. Barret, *J. Am. Ceram. Soc.* **73**, 3319 (1990).

<sup>6</sup>P. Meredith, A.M. Donald, and K. Luke, *J. Mater. Sci.* **30**, 1921 (1995).

<sup>7</sup>H.F.W. Taylor, in *The Chemistry of Cements* (Academic, New York, 1964).

<sup>8</sup>H.F.W. Taylor, in *Cement Chemistry* (Academic, London, 1990).

<sup>9</sup>P. Barnes, *Met. Mater.* **6**, 708 (1990).

<sup>10</sup>P. Barnes, *J. Phys. Chem. Solids* **52**, 1299 (1991).

<sup>11</sup>H. He, P. Barnes, J. Munn, X. Turrillas, and J. Klinowski, *Chem. Phys. Lett.* **196**, 267 (1992).

<sup>12</sup>D. Häusermann and P. Barnes, *Phase Trans.* **39**, 99 (1992).

<sup>13</sup>R. J. Cernik and P. Barnes, *Radiat. Phys. Chem.* **45**, 445 (1995).

<sup>14</sup>P. Barnes, X. Turrillas, A.C. Jupe, S. L. Colston, D. O'Connor, R. J. Cernik, P. Livesey, C. Hall, D. Bates, and R. Dennis, *J. Chem. Soc. Faraday Trans.* **92**, 287 (1996).

<sup>15</sup>E. Henderson, X. Turrillas, and P. Barnes, *J. Mater. Sci.* **30**, 3856 (1995).

<sup>16</sup>P. Barnes, S.M. Clark, D. Häusermann, E. Henderson, and C.H. Fentiman, S. Rashid, and M.N. Muhamad, *Phase Trans.* **39**, 117 (1992).

<sup>17</sup>S. Rashid, P. Barnes, and X. Turrillas, *Adv. Cem. Res.* **4**, 61 (1992).

<sup>18</sup>M.N. Muhamad, P. Barnes, C.H. Fentiman, D. Häusermann, H. Pöllmann, and S. Rashid, *Cem. Concr. Res.* **23**, 267 (1993).

<sup>19</sup>S.M. Clark and P. Barnes, *Cem. Concr. Res.* **25**, 639 (1995).

<sup>20</sup>H.M. Rietveld, *Acta Crystallogr.* **22**, 151 (1967).